X-ray photoelectron spectroscopy (XPS)

Risalat Amir Khan and Niels Schröter

17th November 2011

Abstract

For the present report we conducted XPS experiments on a freshly evaporated film of samarium, a silver sample and a 10 DM commemorative coin. For the samarium film, we identified several characteristic and Auger emissions from samarium and oxygen, from which we conclude that the film was partially oxidised. A closer examination of the characteristic Sm 4s emissions reveals a multiplet splitting of about $\Delta E_{splitt} \approx 5.9eV$ and an intensity ration of the two peaks of $\frac{I(S=\frac{7}{2})}{I(S=\frac{5}{2})} \approx 1.7$, which agrees well with the theoretical predictions. In the silver sample spectrum, we observe several characteristic and Auger emissions from silver and oxygen, and conclude again that the sample surface is oxidised. A superposition of spectra taken with different photon energies reveals three pairs of Auger emissions in sample. The spectra from the 10 DM commemorative coin confirms the compositions of the compound as stated by the Bundesbank, although we conclude that at least parts of the surface are oxidised. Furthermore, a contamination with samarium from a previous experiment has taken place.

1 Introduction

X-ray photoelectron spectroscopy (XPS) uses monochromatic photon radiation to detach electrons from atoms, molecules or solids. From the kinetic energy of the ionized electrons, one can derive information about the electronic structure of the specimen. In the case of condensed matter, only electrons from a thin surface layer of 2-20$\mathring{A}$ are emitted without loss of energy, thus XPS is very surface sensitive. [6]

1.1 Emission mechanisms

In the case of a solid state, an electron can leave the bulk if the energy exceeds the sum of the binding energy of the electron E_B and the workfunction of the solid Φ_s. Due to energy conservation, the resulting kinetic energy of the electron detected in the spectrometer is given as

$$E_{kin} = h\nu - E_B - \Phi \tag{1}$$

where h is Plank's constant, ν is the frequency of the incident photon and $\Phi = \Phi_s + \Phi_{spec}$ is the sum of the workfunctions of the solid and the spectrometer. In this case, E_B is measured relative to the Fermi level E_F. [6]The following processes produce characteristic emissions in the XPS spectrum [10]:

1. Valence band emissions.
2. Inner shell emissions.
3. Auger electron emissions. They are created when an electron is filling an inner shell vacancy and thereby causes the emission of another electron.
4. Satellite Peaks. They are caused by multiple X-ray emission lines in the X-ray source.
5. X-ray ghost lines, coming from contaminations of the X-ray anode, copper from the anode clipping, oxidisation of the anode.
6. Shake up lines, due to the creation of an ion in an excited state.
7. Background emissions. They can be caused by extrinsic losses, where the emitted electron scatters with bulk phonons (secondary electrons, causes continuous emissions), or intrinsic losses (plasmons), where the electron looses a specific amount of energy due to interactions with other electrons (causes discrete background).

1.2 Line splitting and shifts

Due to quantumechanical and chemical effects, the emission peaks in the XPS spectrum can be split or shifted.

Splitting

The splitting of the the emission peaks can be caused by two quantumechanical effects:

1. Spin-Orbit coupling: The spin of an electron couples with its orbital momentum and thereby splits it in multiple states. This does not occur in s states, bacause their angular momentum is zero [6].

2. Multiplet splitting: After the ionization of an electron from an s state, the spin of the remaining electron can couple with the spin of a partially filled state and thereby cause a splitting of the s state[9]. We will deal with this effect in more detail in a following task.

Chemical shift

Due to the formation of metal atoms to compounds, esp. oxides, the screening of the nucleus charge due to inner shell electrons can be broken when these electrons are donated to the partner atom in the compound. Therefore, the binding energy of certain energy levels can be larger in a chemical compound then in the pure metal, which is called the **chemical shift** due to neighbouring atoms [9].

1.3 Instrumentation and spectral resolution

In order to minimize the contamination of the sample surface, the experimental chamber has to be brought under ultra high vacuum conditions. To archive a final pressure of about $10^{-11} mbar$, the VC got pumped with a turbopump and was baked out afterwards. As an X-ray source, anodes out of Magnesium and Aluminium were used without a monochromator, allowing photons with multiple characteristic wavelengths to penetrate the sample. This might cause the appearance of satellite peaks. The samples are attached to a rotatable sample holder, so that different samples can be brought into the optimal angular position between the X-ray source and the electron analyser.

Electron analyser

To measure the kinetic energy of the emitted electrons, the electron beam is focussed on spherical capacitor and detected by channeltron which multiplies the electron signal. A sketch of the set-up is shown in fig. 1.

Before being focussed by an electrical lens, the electrons are retarded by an electrical field, so that only electrons with $E_{kin} > E_{Pass}$ can pass on to the capacitor, where E_{pass} is called the "pass energy". Applying a pass energy has two effects: (i) Reducing the background noise from secondary electrons[6] and (ii) enhancing the resolution of the analyser [9]. Besides the pass energy, the width of the slits is affecting the resolution of the energy analyser.

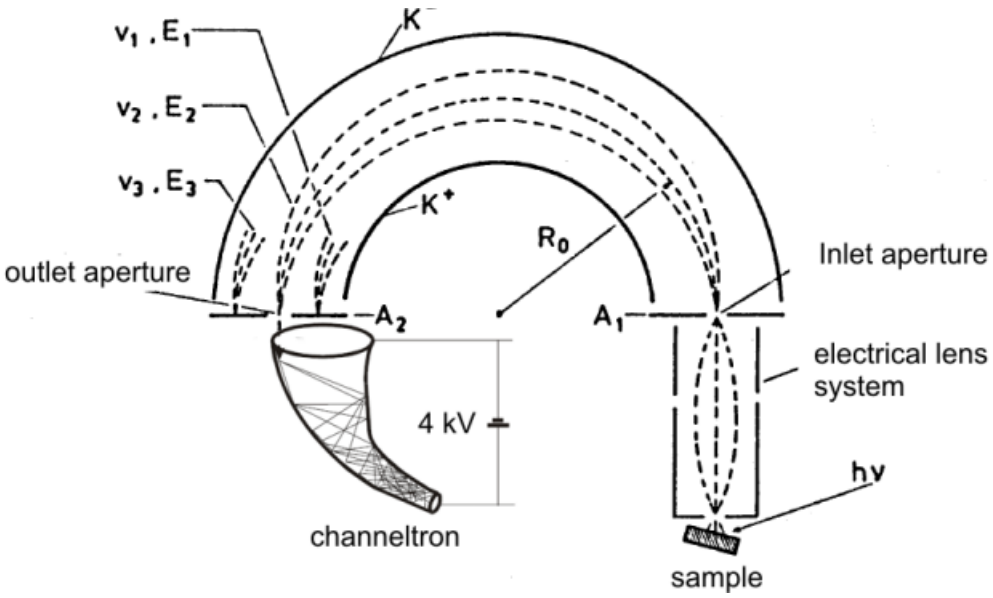

Figure 1: **Sketch of the electron analyser.** Electrons which are emitted from the sample are focused on the spherical capacitor entrance slit by the electrical lens system. In the capacitor, electrons with different energies are spatially separated. Electrons with a predetermined energy can pass the exit slit, their signal is multiplied by the channeltron.

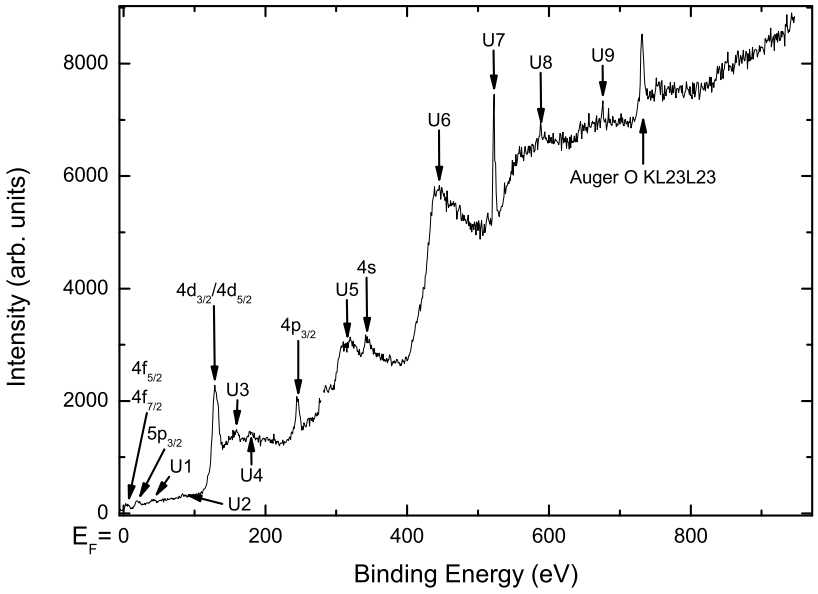

Figure 2: **Overview spectrum of samarium film.** Besides the characteristic emissions from samarium, Auger emissions from oxygen are observed , which suggests that at least parts of the film are already oxidised.

2 Overview spectrum of samarium

2.1 Experimental

After adjusting the the sample holder to the optimal angular position, our tutor started the evaporation and deposition of an samarium film on a steel sheet. Subsequently, we used the Mg-anode to take an overview spectrum of the samarium, setting a pass energy of $E_{pass} = 50eV$, a resulution of $\approx 1\frac{pt}{eV}$, a measurement time of $333\frac{ms}{eV}$ and summing the results of two runs in order to reduce statistical fluctuations.

2.2 Results and Discussion

We located the the Fermi level at $E_F = 1247$ eV, which lies at the upper end of the first significant peak below the photon energy of the $Mg - K_\alpha$ line of 1253 eV [10]. Using eq. 1, we calculated an effective work function of $\Phi \approx 6$ eV and converted the overview spectrum to binding energies, which is shown in fig. 2.

All significant peaks are tabulated in table 1, if they were identified, the reference values are taken from [3, 1, 5, 8].

It is obvious that emissions up to the 4^{th} shell are present, since in the case of samarium the photon energy from the Mg-anode is not high enough to ionize electrons from lower shells. Since emissions that are related to Auger emissions

Spectral line	Formula	Measured E_B/eV	Reference E_B/eV
Sm $4f_{5/2}/4f_{7/2}$	Sm/Sm_2O_3	5±4	5.2
Sm $5p_{3/2}$	Sm	19±3	21.3
U1		42 ± 3	
U2		83 ± 2	
Sm $4d_{3/2}/4d_{5/2}$	Sm	128±4	129
U3		159 ± 4	
U4		180 ± 4	
Sm $4p_{3/2}$	Sm	245±3	247.4
U5		315±10	
Sm $4s$	Sm	344±5	347.2
U6		445±15	
U7		523 ± 2	
U8		589±2	
U9		676±19	
Auger O KL23L23	Sm_2O_3	731±2	731

* the kinetic energy reference values of the Auger emission were converted via eq. 1 in binding energies.

Table 1: **Peak positions and designations from the samarium spectrum.** Reference values are taken from [5, 3, 1, 8].

from oxygen atoms are observed, it is plausible that at least parts of the Sm film were already oxidised when the measurement took place. According to [3], the chemical shift that should be present due to the oxidisation is for all observed lines smaller then the estimated error. Despite our significant efforts, it was impossible for us to identify the peaks numbered as U1-U9 with certainty. Due to their discrete character and proximity to characteristic lines of higher kinetic energy, the lines U1, U2, U3, U4, U8 and U9 might be discrete replications, such as satellite peaks, shake-ups or plasmons. The U5 emissions seems to exhibit a splitting, while the strong emission U7 seems to be caused due to a characteristic emission of an unidentified species. The broad U6 band might be caused by an unidentified characteristic emission, followed by a continuous distribution of electrons with smaller energies due to inelastic scattering with phonons, e.g. the Sm Auger M5N3N67+2 emission at $E_{kin} \approx 802$eV [5].

3 Samarium 4s spectrum

3.1 Experimental

After performing several testruns, we finally applied a measurement with the Mg-anode around the expected position of the 4s emission at 347.2eV[1]: $E_{pass} = 30eV$, resolution$\approx 12.5\frac{pt}{eV}$, measurement time $1500\frac{ms}{eV}$, summing over 5 runs.

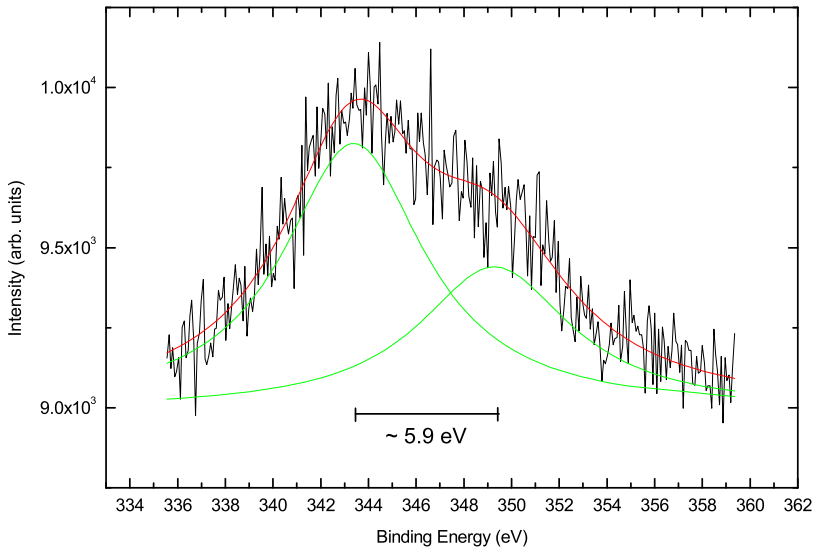

Figure 3: **Samarium 4s multiplet splitting.** Fit was performed with multiple Lorentz curves.

3.2 Results and Discussion

The spectrum around the expected position of the 4s spectrum is shown in fig. 3. We observed a clear splitting of the 4s emission into two lines, which can be explained by the so called "core polarization": Core level photoelectron-emission produces a final core-hole state with spin and angular momentum. If the examined atom has an open valence shell configuration, there can be a coupling between the core-hole orbital and angular momentum that leads to a number of different final states. In present experiment, Samarium has a total valence electron spin of $S = \frac{6}{2}$, after photoionisation in the 4s shell the spin $s = \frac{1}{2}$ of the photohole can couple to the valence spin producing two final states with total spin $J = \frac{5}{2}$ or $J = \frac{7}{2}$. The intensities of the peaks reflect the (2J+1)-degeneracy of the total angular momentum of states. The theoretical ratio between the two 4s peaks of samarium is therefore given as

$$\frac{I(S=\frac{7}{2})}{I(S=\frac{5}{2})} = \frac{2\cdot\frac{7}{2}+1}{2\cdot\frac{5}{2}+1} = \frac{8}{6} \approx 1.3$$

Although theoretically a Vogt curve should fit XPS emissions best [4], it did not converge on our measured spectrum, which might be due to the missing baseline correction. Therefore, we applied a multiple-Lorentz curve fit which converged well and is shown in fig. 3. From the fit, we got an integrated intensity ratio of $\frac{I(S=\frac{7}{2})}{I(S=\frac{5}{2})} \approx 1.7$ which is close to the theoretical value. The splitting was determined as $\Delta E_{splitt} \approx 5.9eV$, which is close to the theoretical value of $0.55eV$ from Hartree-Fock calculations [7].

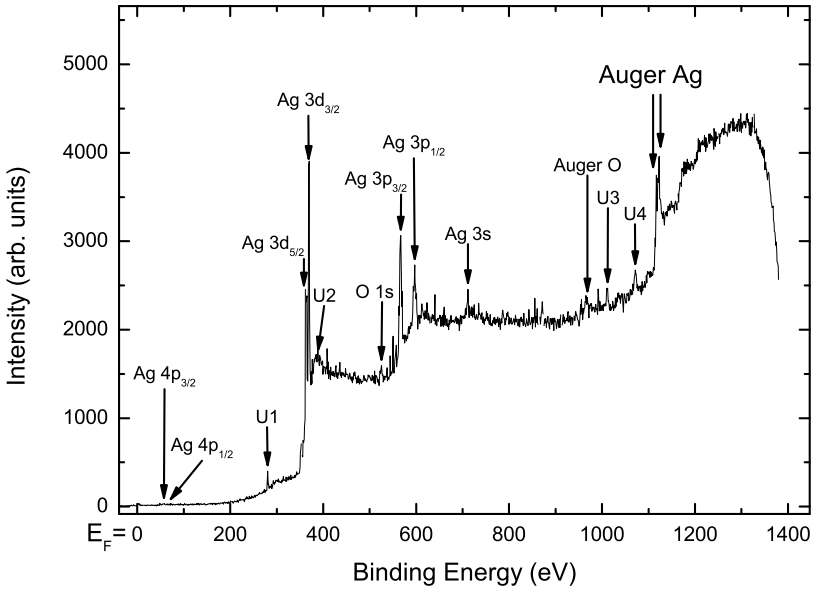

Figure 4: **Overview spectrum of silver sample.** Besides the characteristic and Auger emissions from Ag, characteristic and Auger emissions from oxygen are observed, which suggests that at least parts of the sample are already oxidised.

4 Overview spectrum of silver sample

4.1 Experimental

After adjusting the the sample holder to the optimal angular position for the silver sample, we used the Al-anode to take an overview spectrum. We set a pass energy of $E_{pass} = 30eV$, a resulution of $\approx 1\frac{pt}{eV}$, a measurement time of $333\frac{ms}{eV}$ and summed the results of two runs. For the determination of the Auger peaks we took another overview spectrum with the Mg-anode, using the same configuration.

4.2 Results and Discussion

Like in section 2.2, we determined $E_F \approx 1480$eV, $\Phi \approx 7$eV with an assumed photon energy for the $Al - K_\alpha$line of 1487eV [10]. The overview spectrum is shown in fig. 4, all characteristic peak positions are tabulated in table 2.

Besides multiple characteristic Ag emissions, we observed characteristic emissions from oxygen, which suggests that at least parts of the surface are oxidised. For higher binding energies, the measured values start to deviate from the reference towards lower binding energies, although a chemical shift caused by oxidisation should shift the peaks to higher binding energies [3]. The uniden-

Spectral line	Formula	Measured E_B/eV	Reference E_B/eV
Ag 4p3/2	Ag	57±2	58.3
Ag 4p1/2	Ag	63±2	63.7
Unidentified U1		280±3	
Ag 3d5/2	Ag	364±3	367.90
Ag 3d3/2	Ag	369±3	374.0
Unidentified U2		388 ± 10	
O 1s	AgO	525±5	528.40
Ag 3p3/2	Ag	567±5	573.0
Ag 3p1/2	Ag	596±5	603.8
Ag 3s	Ag	711±5	719.0
Auger O KL23L23	AgO	968±5	966.8*
Unidentified U3		1012±3	
Unidentified U4		1071±4	
Auger Ag M4N45N45	Ag	1117±3	1119.9*
Auger Ag M4N45N45	Ag	1123±4	1123.0*

* the kinetic energy reference values of the Auger emission were converted via eq. 1 in binding energies.

Table 2: **Peak positions and designations from the silver sample spectrum.** Reference values are taken from [5, 3, 1, 8].

tified peaks U2, U3, U4 might be replicas, while U1 seems to be caused by a characteristic emission from an unknown source. The large width of U2 is probably caused by phonon scattering.

The resolution of the full details of the peak structure is influenced by [9, 6]:

1. the pass energy
2. the width of the slits in the energy analyser
3. the diameter of the analyser
4. the photon energy distribution in the X-ray source (here: width of $K_\alpha$lines)

Obviously, certain parts of the spectra cannot be explored because the energy of the incident photons is not high enough cause characteristic emissions in this region. In the present case, no characteristic emissions involving electrons below the 3^{rd} shell could be observed.

In order to determine the position of the Auger peaks, which were above identified from reference values, we superimposed the spectra taken with the Al- and Mg-anode. Because the Auger emission originates from the inner-atomic reordering of the electron shells, its kinetic energy is independent from the energies of the incident photons. Thus, in the superimposed spectrum, their energies should stay at the same position, while the characteristic emissions shift relative to each other according to eq. 1. Fig. 5 shows the superposition of the spectra, the inset shows the enlarged section of the Auger transitions.

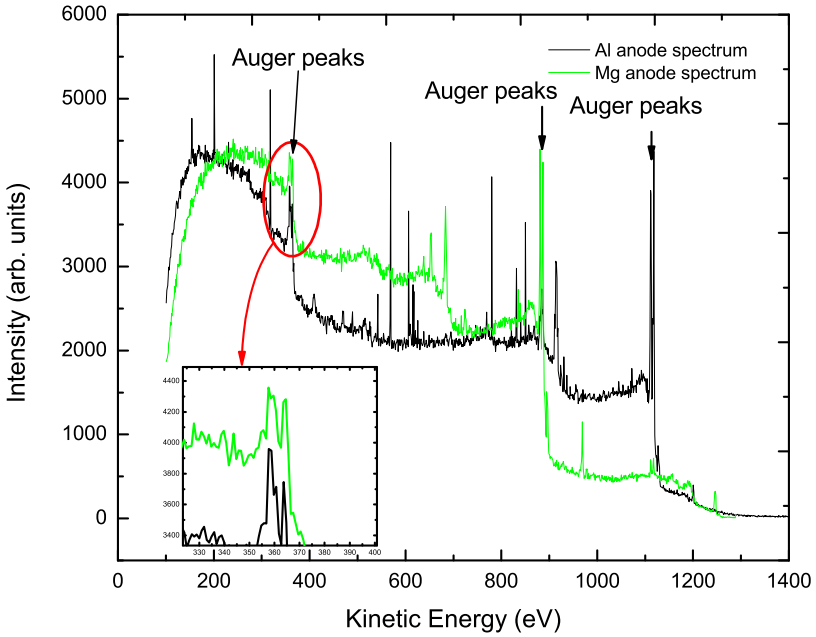

Figure 5: **Superposition of Mg- and Al-anode spectra from silver sample.** Three pairs of Auger transitions can be identified, which are in both spectra at the same position, which is emphasised in the inlet.

From this plot, we determined two Auger kinetic energies at $E_{aug1} = 363 \pm 3eV$ and $E_{aug1} = 357 \pm 4eV$. According to references, they are caused by transitions in silver atoms [3, 5]. Further Auger transitions where observed at $E_{aug3} = 880 \pm 3eV$, $E_{aug4} = 887 \pm 3eV$, $E_{aug5} = 1111 \pm 3eV$, $E_{aug6} = 1117 \pm 3eV$. These transitions could not be traced to a specific transition. It is suspicious that all six Auger emissions appear in pairs of two peaks with about the same spacing between each pair. This suggests that the peaks at lower energies are replicas of the ones with higher energies.

5 10 DM commemorative coin

5.1 Experimental

We found the commemorative coin filed and mounted on the sample holder, which we adjusting to the optimal angular position. Subsequently, we used the Mg-anode to take an overview spectrum of the commemorative coin. We set a pass energy of $E_{pass} = 30eV$, a resulution of $\approx 1\frac{pt}{eV}$, a measurement time of $333\frac{ms}{eV}$ and summed the results of three runs.

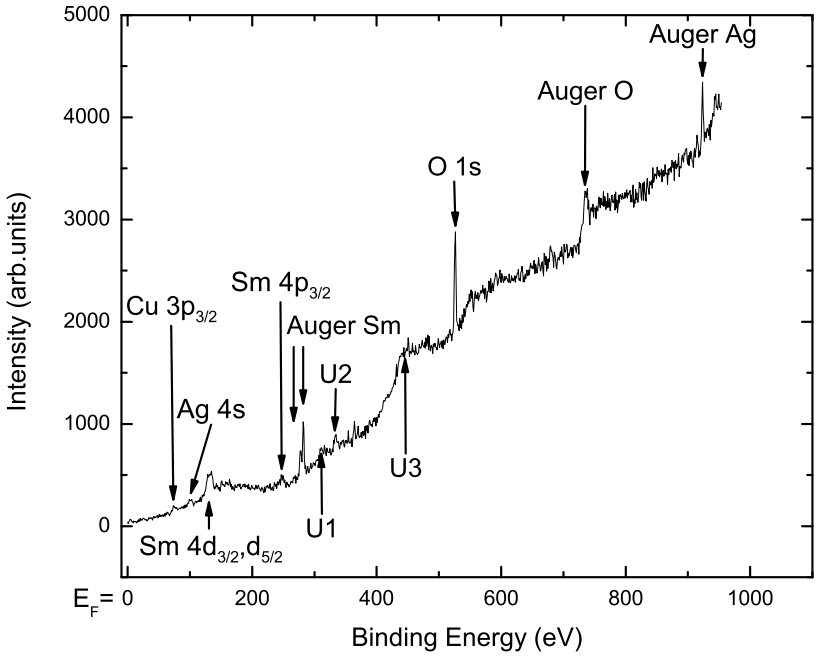

Figure 6: **Overview spectrum of commemorative coin.** Besides the characteristic and Auger emissions from Ag and Cu, characteristic and Auger emissions from oxygen are observed, which suggests that at least parts of the coin surface is already oxidised. Emissions from samarium suggest a contamination during the evaporation in the previous task.

5.2 Results and Discussion

Like in section 2.2, we determined $E_F \approx 1248$eV and $\Phi \approx 5$eV . The overview spectrum is shown in fig.6, all characteristic peak positions are tabulated in table 3.

According to the Bundesbank, the 10 DM commemorative coin consists out of a binary alloy of silver and copper [2]. Our results confirm this statement, since we found characteristic and Auger emissions from copper and silver, although the presence of emissions originating from oxygen suggest that at least parts of the surface is oxidised. In addition to the aforementioned emissions, we found characteristic and Auger emissions from samarium, which suggests that at the coin was contaminated during the evaporation of samarium for the first task. Once again, we observed a pair of emissions at $E_B = 281eV/277eV$, which we designated to an Auger emission from samarium, although in hindsight of the suspicious Auger transitions in the silver sample (section 4.2), which also appeared in pairs of two, this designation cannot made with certainty. The emissions from the unidentified lines at U1 and U2 might be replicas of lines with higher energy, while U3 seems to have the same lineshape as the emission

Spectral line	Formula	Measured E_B/eV	Reference E_B/eV
Auger Ag M1M5N45	Ag/AgO	922 ± 1	922.5*
Auger O KL23L23	AgO	734 ± 3	731*
U3		446 ± 14	
O 1s	AgO	525 ± 2	528.40
U2		333 ± 3	
U1		310 ± 2	
Auger Sm M4N45N67+2	Sm	281 ± 1	277*
Auger Sm M4N45N67+2	Sm	277 ± 2	277*
Sm 4p3/2	Sm	246 ± 2	247.4
Sm 4d 3/2,5/2	Sm	131 ± 6	131
Ag 4s	Ag	99 ± 2	97.40
Cu 3p3/2	Cu	73 ± 2	75.10

* the kinetic energy reference values of the Auger emission were converted via eq. 1 in binding energies.

Table 3: **Peak positions and designations from the commemorative coin spectrum.** Reference values are taken from [5, 3, 1, 8].

U6 in the samarium overview spectrum. As mentioned before, both bands might originate in an Auger transition which produced a continuous background due to inelastic phonon scattering.

References

[1] Center for x-ray optics and advanced light source, x-ray data booklet, technial and electical information department - lawrence berkeley national laboratory, berkeley (2001).

[2] Gedenkmünzen der bundesrepublik deutschland 10 dm. Deutsche Bundesbank, `http://www.bundesbank.de/download/bargeld/pdf/euro_dm_gedenkmuenzen10.pdf` [12.11.2011].

[3] Nist x-ray photoelectron spectroscopy database, version 3.5 (national institute of standards and technology, gaithersburg, 2003); http://srdata.nist.gov/xps/ [12.11.2011].

[4] Matthias Bernien. *X-Ray Absorption Spectroscopy of Fe Complexes on Surfaces: Electronic Interactions and Tailoring of the Magnetic Coupling.* PhD thesis, Freie Universität Berlin, 2009.

[5] W.A. Coghlan and R.E. Clausing. Auger catalog calculated transition energies listed by energy and element. *Atomic Data and Nuclear Data Tables*, 5(4):317 – 469, 1973.

[6] Freie Universität Berlin. *Script: Ma4: X-ray photoelectron spectroscopy (XPS), Freie Universität Berlin.*

[7] A. Rosencwaig H.J. Guggenheim G.K. Wertheim, R.L. Cohen. Multiplet splitting and two-electron excitation in the trivalent rare earths. Electron Spectroscopy, S. 813, Ed. D.A. Shirley, North-Holland, 1972.

[8] K. Goto, N. Sakakibara, Y. Takeichi, Y. Numata, and Y. Sakai. True auger spectral shapes: A step to standard spectra. *Surface and Interface Analysis*, 22(1-12):75–78, 1994.

[9] S. Hüfner. *Photoelectron spectroscopy: principles and applications*. Springer series in solid-state sciences. Springer, 2003.

[10] Mike Bancroft Igor Bancroft Igor Bello & Friends Roger Smart, Stewart McIntyre. X-ray photoelectron spectroscopy, lecture notes. Department of Physics and Materials Science, City University of Hong Kong, `http://mmrc.caltech.edu/SS_XPS/XPS_PPT/XPS_Slides.pdf` [03.11.2011].